NeuroImage: Clinical 25 (2020) 102109

Contents lists available at ScienceDirect

NeuroImage: Clinical

journal homepage: www.elsevier.com/locate/ynicl

REVIEW: MR elastography of brain tumors

Adomas Bunevicius[a,b], Katharina Schregel[c], Ralph Sinkus[d], Alexandra Golby[a,b,e], Samuel Patz[b,e,*]

[a] Department of Neurosurgery, Brigham and Women's Hospital, Boston, MA 02115, United States
[b] Harvard Medical School, Boston, MA, United States
[c] Institute of Neuroradiology, University Medical Center Goettingen, Goettingen, Germany
[d] Inserm U1148, LVTS, University Paris Diderot, University Paris 13, Paris, France
[e] Department of Radiology, Brigham and Women's Hospital, Boston, MA 02115, United States

ARTICLE INFO

Keywords:
MR elatography
Brain tumor
Glioma
Meningioma
Pituitary adenoma
Surgical planning

ABSTRACT

MR elastography allows non-invasive quantification of the shear modulus of tissue, i.e. tissue stiffness and viscosity, information that offers the potential to guide presurgical planning for brain tumor resection. Here, we review brain tumor MRE studies with particular attention to clinical applications. Studies that investigated MRE in patients with intracranial tumors, both malignant and benign as well as primary and metastatic, were queried from the Pubmed/Medline database in August 2018. Reported tumor and normal appearing white matter stiffness values were extracted and compared as a function of tumor histopathological diagnosis and MRE vibration frequencies. Because different studies used different elastography hardware, pulse sequences, reconstruction inversion algorithms, and different symmetry assumptions about the mechanical properties of tissue, effort was directed to ensure that similar quantities were used when making inter-study comparisons. In addition, because different methodologies and processing pipelines will necessarily bias the results, when pooling data from different studies, whenever possible, tumor values were compared with the same subject's contralateral normal appearing white matter to minimize any study-dependent bias. The literature search yielded 10 studies with a total of 184 primary and metastatic brain tumor patients. The group mean tumor stiffness, as measured with MRE, correlated with intra-operatively assessed stiffness of meningiomas and pituitary adenomas. Pooled data analysis showed significant overlap between shear modulus values across brain tumor types. When adjusting for the same patient normal appearing white matter shear modulus values, meningiomas were the stiffest tumor-type. MRE is increasingly being examined for potential in brain tumor imaging and might have value for surgical planning. However, significant overlap of shear modulus values between a number of different tumor types limits applicability of MRE for diagnostic purposes. Thus, further rigorous studies are needed to determine specific clinical applications of MRE for surgical planning, disease monitoring and molecular stratification of brain tumors.

Introduction

Surgery is the principal therapy in the management of both benign and malignant brain tumors. Benign brain tumors, such as meningiomas and pituitary adenomas, can be cured with gross total tumor resection. Despite inevitable disease progression and clinical deterioration, patients with gliomas also benefit from resection of the maximally safe tumor volume both at the time of initial presentation and after progression of the tumor (Almenawer et al., 2015; Lu et al., 2018; Xia et al., 2018). Careful pre-operative planning is critical for maximally safe tumor resection and optimal treatment outcome. Knowledge of brain tumor mechanical stiffness is of potential importance for presurgical planning as it might help to determine the best surgical approach, instrument selection, and tumor resection strategy, and has been linked to postoperative complication risk and extent of resection (Itamura et al., 2018; Zada et al., 2013, 2011). Shear wave ultrasound elastography has proven to be a valuable tool for assessment of brain tumor stiffness intraoperatively but since a bone window is required (Chauvet et al., 2016), its use for pre-operative planning is precluded.

The armamentarium of non-invasive imaging modalities for brain tumor diagnosis, surgical planning, intra-operative imaging and monitoring of treatment response is constantly growing. Studies using Magnetic Resonance Imaging (MRI) or Computed Tomography (CT) have been performed to estimate brain tumor stiffness. MRI studies have included both anatomical T2-weighted MRI scans to estimate meningioma stiffness (Shiroishi et al., 2016) as well as diffusion

* Corresponding author at: Department of Radiology, Brigham and Women's Hospital, Boston, MA 02115, United States.
E-mail addresses: a.bunevicius@yahoo.com (A. Bunevicius), patz@bwh.harvard.edu (S. Patz).

https://doi.org/10.1016/j.nicl.2019.102109
Received 2 October 2019; Received in revised form 19 November 2019; Accepted 22 November 2019
Available online 23 November 2019

weighted MRI for the estimation of pituitary adenomas stiffness (Yiping et al., 2016). The results from these studies, however, has either been inconclusive or inconsistent. Greater stiffness of vestibular schwannomas was linked to greater internal auditory canal widening as observed with head CT but did not correlate with signal intensity on T2 weighted MRI (Rizk et al., 2017). These findings indicate that pre-operative estimation of brain tumor stiffness via conventional imaging is suboptimal and that new noninvasive methods are needed.

Magnetic Resonance Elastography (MRE) provides a direct quantitative measure of the tissue shear modulus. This includes both the shear stiffness and shear viscosity, both of which may be highly relevant for predicting the ease of tumor resectability and that, in turn, can be important for pre-surgical planning. MRE is an MRI based imaging technique that allows quantification of the tissue shear modulus **G*** in vivo by measuring the propagation of mechanical shear waves induced by a vibration device held against the surface of the body (Muthupillai et al., 1995). MRE, which applies a motion encoding gradient (MEG) to produce a phase shift associated with the shear wave harmonic motion, has been adapted to many different types of pulse sequences, i.e. spin echo, gradient echo, EPI. The application of mechanical vibrations to the brain is well tolerated and of no significant risk. For example, the amplitude of the vibrations is extremely small, on the order of 100 μm or less, and the frequency of vibration typically ranges from ~30–80 Hz (imagine an electric toothbrush held against your head). The shear modulus **G*** has two components expressed as the real and imaginary components of the complex quantity **G*** = G' + iG". Here G' is the shear stiffness also known as the elasticity or storage modulus and G" is the shear viscosity also known as the loss modulus. For a physical interpretation of these terms, consider a spring with a weight attached. The "stiffness" (G') of the spring is inversely related to the extension of the spring when the weight is attached. Any decrease in amplitude associated with harmonic motion of the mass will incur losses and these losses are related to G". For shear waves in tissue, the stiffness G' is mainly reflected in the wavelength of the traveling mechanical waves. Increasing stiffness results in shear waves traveling faster and hence with an increase in wavelength (**Fig. 1**). The viscosity G" is related to losses and is mainly reflected in the attenuation of the waves as they travel through a medium. The phase angle φ is defined as the angle whose tangent is the ratio G"/G' (**Fig. 1c**). It is important to appreciate the different components of **G*** as different studies report their data differently and when comparing data between different studies, one must ensure that similar quantities are being compared. For example, some studies report magnitude $|G^*|=\sqrt{(G')^2 + (G'')^2}$ and phase angle φ, while other studies only report the shear stiffness (G').

Regarding current clinical use of MRE, it is considered the most accurate non-invasive method for quantification of liver fibrosis (Expert Panel on Gastrointestinal Imaging: et al., 2017; Kim et al., 2018). Other potential clinical applications, including both oncologic and non-oncologic disorders, are promising but remain under investigation. For example, MRE has been studied in non-CNS malignancies, including prostate cancer (Li et al., 2011), hepatocellular cancer (Thompson et al., 2017) and breast cancer (Siegmann et al., 2010). More recently, brain MRE of degenerative and other neurological disorders has been investigated (Hiscox et al., 2016; Murphy et al., 2017). Importantly, there is a growing body of evidence suggesting that MRE may be a valuable imaging modality for non-invasive quantification of brain tumor stiffness. MRE could serve as practical method for assessment of brain tumor stiffness as it provides an objective quantitative spatial map of tumor stiffness. Hence, our aim here is to critically review existing brain MRE literature with particular attention to potential clinical applications in patients with brain tumors. In reviewing MRE studies in patients with brain tumors, we pool the data with the goal of determining what sort of consensus existing studies provide in terms of (i) determining the relative stiffness and viscosity of brain tumors compared to normal appearing white matter (NAWM), (ii) whether the data supports the use of MRE to distinguish between different tumor types, and (iii) what MRE parameters, if any, are most sensitive to pathology.

2. Methods

2.1. Systematic review

A systematic literature review was performed on July 21, 2019 to identify studies that performed MRE in patients with a diagnosis of brain tumor. Articles for review were selected from the Pubmed/MEDLINE database by using the following query: ("mr elastography" or "elastography") AND ("brain tumor" or "glioma" or "glioblastoma" or "meningioma" or "pituitary adenoma" or "vestibular schwannoma"). There were no restrictions regarding year of publication; however, a systematic analysis was only performed on literature with human data and where either the abstract and/or full-text was written in English. Review papers and single case reports were excluded from the analysis. Identified papers were also reviewed for references to other relevant studies that employed MRE in brain tumors. An initial literature search was performed by reviewing titles and abstracts of papers, and relevant full-text articles were extracted for further analysis. Full-text articles of selected studies were reviewed for year of publication, study inclusion criteria, study design, number of patients studied and MRE techniques, including MRI field strength and wave generation method. A Flow-Chart summarizing the above-described algorithm to select publications is provided in **Fig. 2**.

Different groups performing brain MRE use different pulse sequences to acquire the data, different devices to vibrate the brain and different inversion algorithms to convert the measured spatial displacement data (acquired as a function of mechanical wave phase) to reconstructed values of the shear modulus. In addition, some groups assume that G" = 0, which simplifies the reconstruction but will also give a different value of G' compared to the case where one does not make this assumption. In addition, the reconstructed values of G are influenced by the signal to noise ratio (SNR) of the measurement. The SNR is influenced by field strength, gradient strength of the motion encoding gradients, and efficiency of mechanical coupling between the vibration device and the subject's head. All of these factors can influence the absolute value of the reconstructed shear modulus. Therefore, in the analysis presented here where data between different groups is compared, not only do we present comparisons of the absolute value of shear modulus indexes but also, to the extent possible, we compare values measured in the tumor relative to contralateral NAWM in the same subject. This comparison, where an internal reference is used in each subject and only differences between G_{tumor} and G_{NAWM} are reported, will essentially remove confounding effects associated with absolute shifts in the shear modulus values from one study to another. While we don't expect large differences in the absolute value of G between different groups, these differences can be sufficiently large to affect differentiation between NAWM and tumor. Therefore, to the extent possible, it is important to measure shear modulus differences with an internal control, i.e. contralateral normal appearing white matter.

Table 1 presents a summary of studies resulting from our literature review. Note that not all studies provided raw shear modulus data for brain tumors and contralateral NAWM. And as mentioned above, some studies ignored any viscous effects in their reconstruction algorithm and hence only reported values for an effective stiffness. To enable a comparison between these studies and those studies that reported magnitude $|G^*|$ and phase φ, we therefore calculated $G' = |G^*|\cos(\varphi)$. Hence for the comparison of the real part of the shear modulus G' for a particular tumor type, we were able to use values from all studies that provided raw data. The complex shear modulus has two independent values and can be represented either in the classical sense of G' and G" (rectilinear coordinates) or as $|G^*|$ and φ (cylindrical coordinates). In

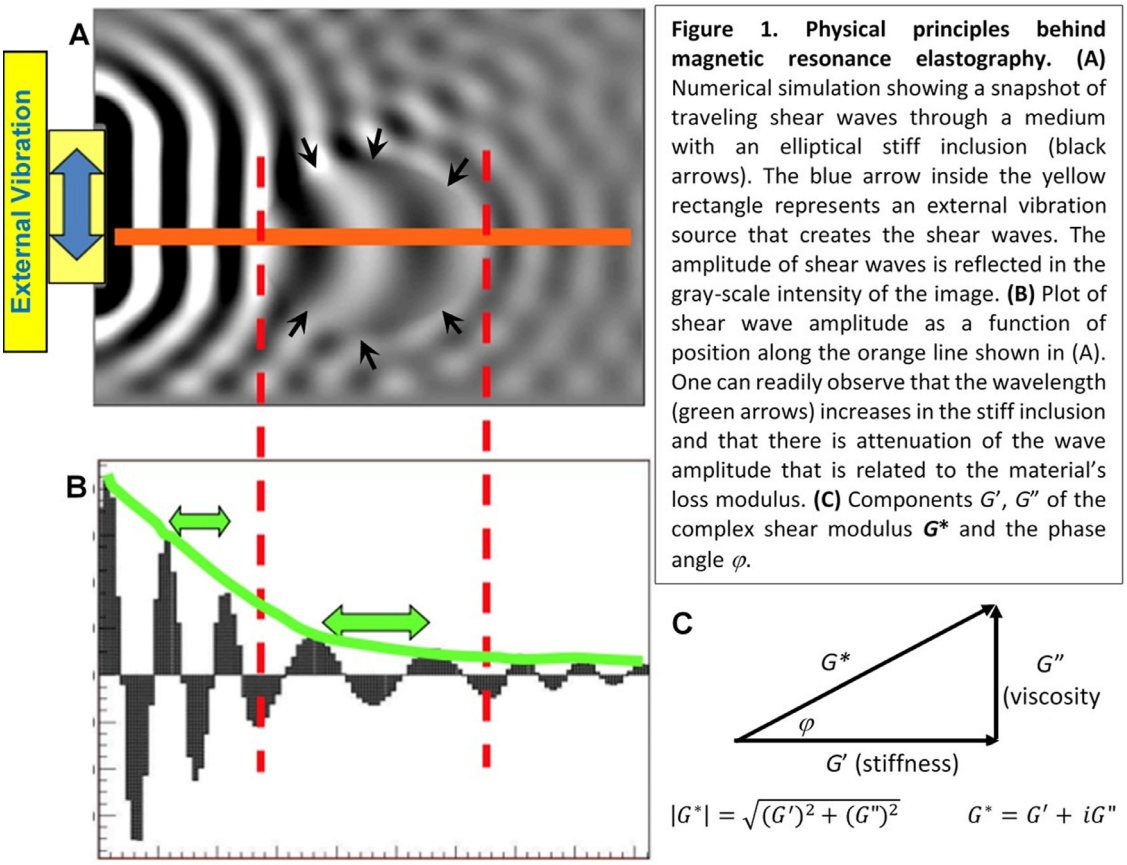

Figure 1. Physical principles behind magnetic resonance elastography. (A) Numerical simulation showing a snapshot of traveling shear waves through a medium with an elliptical stiff inclusion (black arrows). The blue arrow inside the yellow rectangle represents an external vibration source that creates the shear waves. The amplitude of shear waves is reflected in the gray-scale intensity of the image. **(B)** Plot of shear wave amplitude as a function of position along the orange line shown in (A). One can readily observe that the wavelength (green arrows) increases in the stiff inclusion and that there is attenuation of the wave amplitude that is related to the material's loss modulus. **(C)** Components *G′*, *G″* of the complex shear modulus ***G**** and the phase angle φ.

Fig. 1. Flow-chart of study selection.

our comparative analysis, we investigated these two different ways of representing the data to determine which parameters, if any, were superior in terms of differentiating between tumor types or between tumor and NAWM.

2.2. Data Compilation and statistical analyses

First, in Fig. 3, we present pooled data for the absolute value of the shear modulus parameters for each of five different types of tumor as well as NAWM. NAWM was defined in each study as brain areas not affected by tumor in a similar region of the brain but located in the contralateral hemisphere. Next when NAWM data was available, we computed the percentage difference of each shear modulus parameter (ΔG', ΔG", Δ|G*| and Δϕ) to the same subject's NAWM, i.e. using the individual subject's NAWM as an internal control (**Fig. 4 and Table 2**).

Between-group comparisons of mean values were performed using one-way ANOVA analyses and Tukey test was used for post-hoc ANOVA analyses. Results of the ANOVA analyses are presented as the F statistic [degrees of freedom] and p-value, with greater F value indicating greater probability that individual groups are different from each other. Overlap coefficients of shear modulus parameters were calculated for glioblastoma, meningioma, metastatic brain tumor and NAWM.

Statistical analyses were performed using the SPSS Version 19 software (IBM Corp., Armonk, NY) and JMP Version 14 (SAS Institute Inc., Cary, NC).

3. Results

We identified nine studies that performed MRE in a total of 184 primary and metastatic brain tumor patients with sample sizes ranging from 6 (Xu et al., 2007) to 34 (Sakai et al., 2016) patients (**Fig. 2**). The most commonly studied brain tumors were gliomas and meningiomas, followed by pituitary adenomas and metastatic brain tumors. All studies were cross-sectional. For each study, the type of transducer and field strength at which the data was collected is listed in **Table 1**.

3.1. Summary of individual studies without pooling data from different studies

Four studies compared MRE results across different types of brain tumors (Reiss-Zimmermann et al., 2015; Sakai et al., 2016; Simon et al., 2013; Xu et al., 2007). Study sample sizes ranged from 4 (Xu et al., 2007) to 34 (Sakai et al., 2016) patients. One study compared mean ($\overline{G'}$) and maximal (G'_{max}) shear stiffness across meningioma (n = =13), pituitary adenoma (n = =12), vestibular schwannoma (n = =6) and glioma (n = =4) patients (Sakai et al., 2016). They found that both the maximum and mean stiffness values, G'_{max} and $\overline{G'}$ respectively, were greater in meningiomas relative to pituitary adenomas. G'_{max} and $\overline{G'}$ also correlated positively with the intraoperative impression of tumor consistency (Spearman R^2 of 0.25 and 0.18, respectively) as measured on a 5-point scale with greater score indicative of more firm tumors. We note that the term "consistency" is often used in the literature to describe the intraoperatively measured impression of a tumor's mechanical properties. Hence this is both a qualitative and subjective parameter.

A study by Reiss-Zimmermann et al. in patients with glioblastoma (n = 11), anaplastic astrocytoma (n = 3), meningioma (n = 7) and cerebral metastasis (n = 5) found that $|G^*|_{tumor}/|G^*|_{NAWM}$ ratios were similar across different brain tumors. However, meningiomas were clearly distinguishable from other brain tumors by higher $\varphi_{tumor}/\varphi_{NAWM}$ values, while all malignant brain tumors had similar $\varphi_{tumor}/\varphi_{NAWM}$ values (Reiss-Zimmermann et al., 2015). In this study, region of interest (ROI)s over the entire tumor region were defined in consensus reading by three experienced neuroradiologists using T2w, FLAIR and T1w contrast-enhanced images, and G* and φ values within the ROI

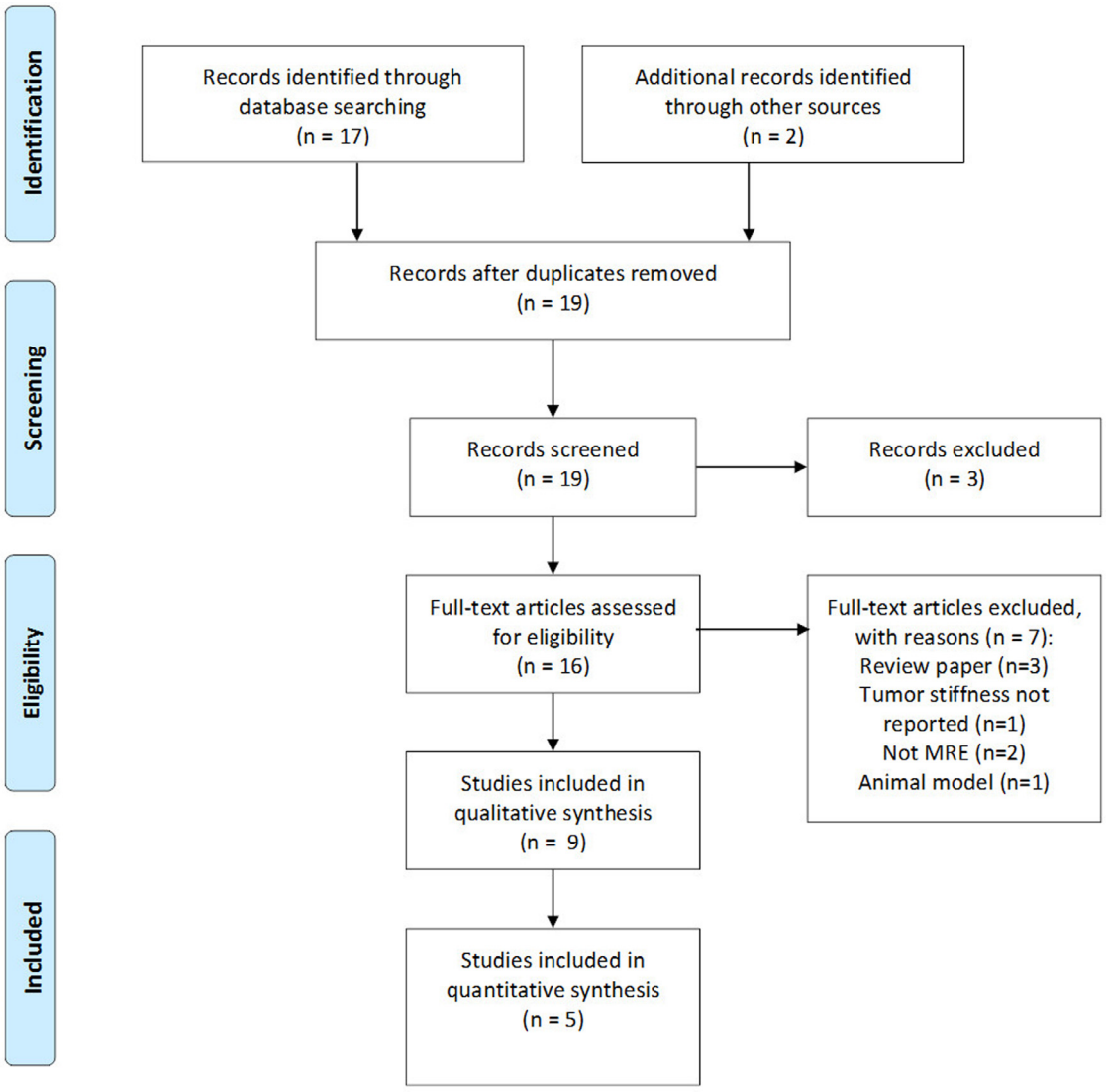

Fig. 2. Studies were selected from the following search terms: Pubmed query: ("mr elastography" or "elastography") AND ("brain tumor" or "glioma" or "glioblastoma" or "meningioma" or "pituitary adenoma" or "vestibular schwannoma").

were averaged.

Another group studied the magnitude |G*| and phase angle φ of the complex shear modulus in 16 patients with various histological types of brain tumors that included gliomas ($n = 10$), brain metastases ($n = 3$), meningiomas ($n = 2$) and lymphoma ($n = 1$) (Simon et al., 2013). Due to small sample sizes across diagnostic categories, their analyses were mainly qualitative. However, the authors noted that mean magnitude |G*| was the lowest in glioblastomas and highest in meningiomas, while the mean phase angle φ was lowest in metastases and greatest in meningiomas. Ratio of magnitude $G^*|_{tumor}/\ |G^*|_{NAWM}$ values were greater than one in both meningiomas and lower than one in other primary intra-axial brain tumors.

A small study in patients with meningiomas ($n = 4$), hemangiopericytoma ($n = 1$), and schwannoma ($n = 1$) reported a qualitative correlation of MRE-measured tumor stiffness relative to the patient's normal white matter and an intraoperative subjective assessment of the same by an experienced neurosurgeon who was blinded to MRE results (Xu et al., 2007). However, neither shear modulus values nor reconstruction methods were reported.

3.2. Gliomas

Two studies investigated MRE in a total 40 glioma patients exclusively (Pepin et al., 2018)(Streitberger et al., 2014). Streitberger and colleagues applied multislice multifrequency MRE (MMRE) to study tumor elastic properties of 22 glioblastoma patients (Streitberger et al., 2014). The MMRE allows the acquisition of 3D wave fields at multiple vibration frequencies. As long as the shear modulus is relatively constant over the range of frequencies used, this can be advantageous in obtaining good quality data over the entire field of view since there may be low displacement amplitude of the shear waves at particular locations for a particular frequency that can be compensated for by using a different frequency. The brain stiffness maps demonstrated that glioblastomas were heterogenous and composed of stiff and soft compartments. Mean |G*| was lower in glioblastomas than unaffected brain parenchyma; however, 5 out of 22 tumors has greater |G*| values than the reference tissue. All glioblastomas had $\varphi_{tumor}/\varphi_{NAWM}$ of less than one, and 17 out of 22 glioblastomas had $|G^*|_{tumor}/\ |G^*|_{NAWM}$ of less than one. Neither φ nor |G*| correlated with the morphologic appearance of gliomas as classified based on preoperative MRI T2-weighted and contrast enhanced T1-weighted images as either homogenous appearing mass, cysts or necrosis/hemorrhage.

Table 1
MRE studies that were identified in patients with brain tumors.

Authors year	# Subjects (# women) / age range	Histological diagnosis (N)	Tumor consistency measured intraoperatively	MRI Field (T) MRE vibration frequency (Hz) vibration apparatus	Major findings
Various histological diagnoses of brain tumors					
Sakai et al., (2016)	34 (23) / range from 14 to 94 years	Meningioma (13), pituitary adenoma (11), vestibular schwannoma (6) and glioma (4)	Yes	3T / 60 Hz (passive pneumatic driver)	G'_{max} and $\overline{G'}$.: meningiomas > pituitary adenomas. Intraoperative consistency of meningiomas correlated with G'_{max}, but not $\overline{G'}$. Intraoperative consistency of meningiomas and all tumors correlated positively with G'_{max}, and $\overline{G'}$Firm tumors had higher G'_{max}, but not $\overline{G'}$ than non-firm tumors.
Reiss-Zimmermann et al. (2015)	27 / range from 36 to 86 years	Glioblastoma (11), anaplastic astrocytoma (3), meningioma (7), cerebral metastasis (5) and intracerebral abscess (1).	No	3T / 30–60 Hz (custom designed cradle)	Authors measured mean values $\|G^*\|$ and φ of tumor and contralateral NAWM. Ratios of $\|G^*\|_{tumor}$/ $\|G^*\|_{NAWM}$ were similar across all studied brain tumors. Meningiomas were clearly distinguishable from other brain tumor using the $\varphi_{tumor}/\varphi_{NAWM}$ that was greater than one in all meningiomas and lower than one in all malignant intra-axial brain tumors.
Simon et al. (2013)	16 (11) / range from 28 to 78 years	Glioblastoma (3), anaplastic astrocytoma (3), low-grade glioma (4), meningioma (2), lymphoma (1), brain metastases (3)	No	3T / 45 Hz (head-cradle driver)	Performed qualitative comparison of mean tumor and contralateral NAWM $\|G^*\|$ and φ. $\|G^*\|$ was the lowest in glioblastoma and the highest in meningioma. φ was the lowest in metastasis and highest in meningioma. $\|G^*\|_{tumor}$/ $\|G^*\|_{NAWM}$ values were greater in meningiomas and lower in other brain tumors.
Xu et al. (2007)	6 (4) / range from 16 to 63 years	Meningioma (4), hemangiopericytoma (1), schwannoma (1)	Yes	3T / 150 Hz (custom-made)	Elasticity of tumors evaluated by the MRE agreed with intra-operative tumor consistency.
Gliomas only					
Streitberger et al. (2014)	22 (10) / range from 18 to 86 years	Glioblastoma multiforme (all patients)	No	1.5T or 3T MRI scanner / 30 to 60 Hz (custom-made head cradle)	Glioblastomas were composed of stiff and soft compartments. Mean $\|G^*\|$ was lower in glioblastomas than unaffected brain parenchyma; however, 5 out of 22 tumors has greater $\|G^*\|$ values than reference tissue. φ was reduced in brain tumors regardless of $\|G^*\|$. All tumors had $\varphi_{tumor}/\varphi_{NAWM}$ of less thann one, and 17 tumors had $\|G^*\|_{tumor}$/ $\|G^*\|_{NAWM}$ of less than one. φ and $\|G^*\|$ did not correlate with tumor size and morphologic appearance on MRI.
Pepin et al. (2018)	18 (6) / range from 25 to 68 years	WHO grade II (5), grade III (7), grade IV (6).	No	3T / 60 Hz (custom-built soft, pillow-like passive driver)	Mean $\|G^*\|$ was lower in glioblastomas when compared to contralateral NAWM. Mean $\|G^*\|$ was lower in grade IV gliomas than in grade II gliomas. $\|G^*\|$ did not correlate with glioblastoma location, patient age, and tumor volume. 12 tumors had IDH-R132H mutation. Gliomas with an IDH1 mutation had greater $\|G^*\|$ than IDH1 wild-type gliomas.
Meningiomas only					
Murphy et al. (2013)	12 / not reported	Meningiomas	Yes	3T / 60 Hz (soft, pillow-like driver)	Tumor $\overline{G'}$ and the ratio of tumor to the surrounding brain tissue $\overline{G'}$ correlated positively with the surgeons' qualitative assessment of tumor stiffness.
Hughes et al. (2015)	14 (10) / range from 28 to 76 years	Meningiomas >2 cm in diameter	Yes	3T / 60 Hz (soft, pillow-like pneumatic driver)	Tumor $\overline{G'}$ correlated positively with surgeons' impression of tumor stiffness and durometer measurements. Sensitivity, specificity and positive predictive values of $\overline{G'}$ for meningioma heterogeneity, homogeneity and hardness were high.
Pituitary adenoma only					
Hughes et al. (2016)	10 (5) / range from 22 to 78 years	Pituitary macroadenomas with maximal diameter of 3.5 ± 0.9 cm [range from 2.5 to 5.2 cm]	Yes	3T / 60 Hz (pillow-like pneumatic driver)	Mean $\overline{G'}$ of soft tumors were lower when compared to intermediate tumors (assessed intraoperatively).

$\overline{G'}$, mean shear stiffness; G'_{max}, maximal shear stiffness; G", shear viscosity; G*, shear modulus; φ, phase angle; MRE, magnetic resonance elastography; NAWM, normal appearing white matter.

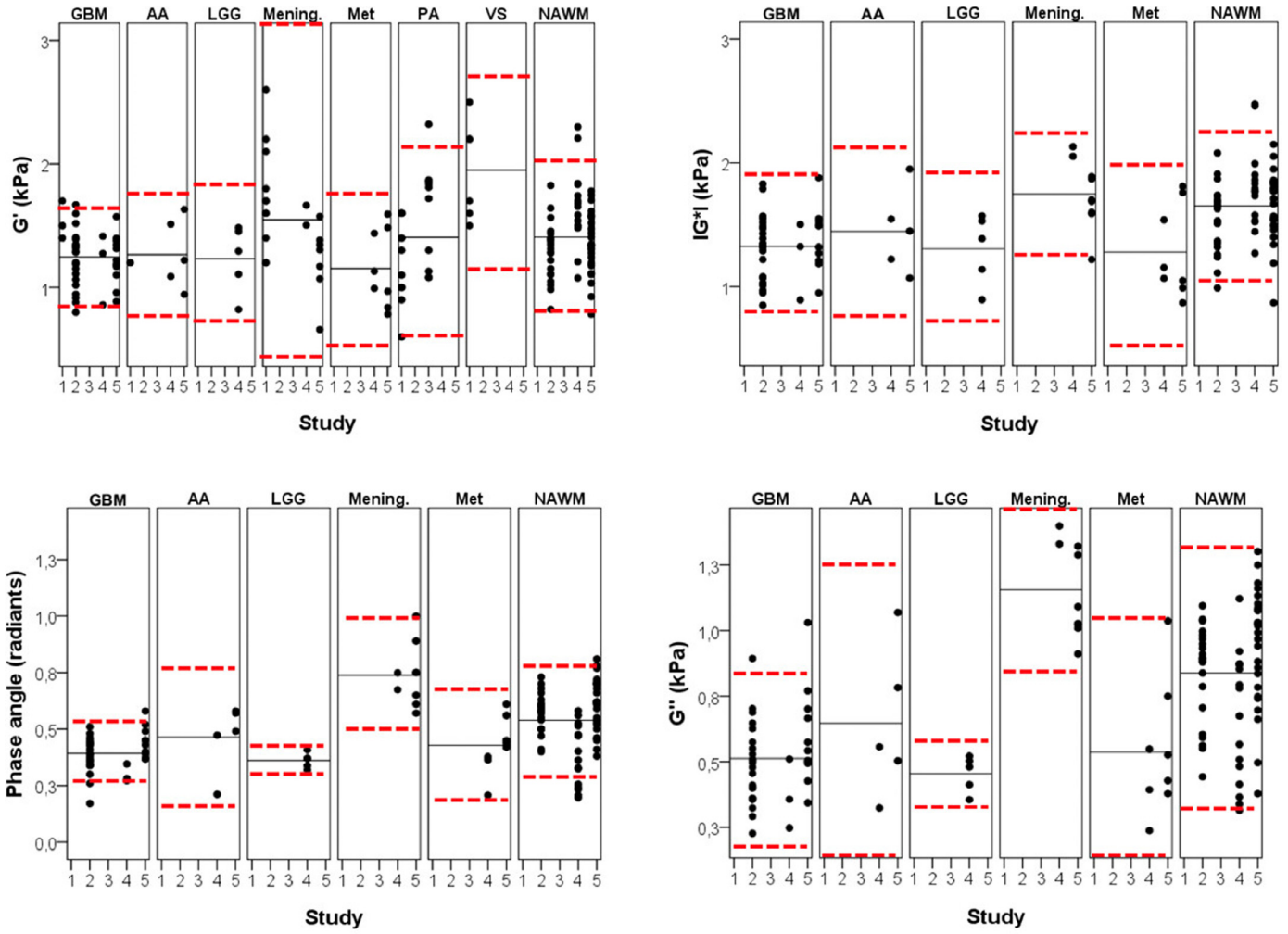

Fig. 3. Plots of (A) G', (B) G", (C) |G*| and (D) phase angle φ from studies from five different groups. The black solid and red dotted horizontal lines correspond to the mean and mean ± 2 standard deviations (SDs) respectively after pooling all data for a particular tumor together. Note that ± 2 SD's equal the 95% confidence interval. Abbreviations are: GBM = glioblastoma; AA = anaplastic astrocytoma; LGG = low grade glioma; Mening. = meningioma; Met = metastatic tumor; NAWM = normal appearing white matter.

Pepin and colleagues studied the association of magnitude |G*| with WHO grade and *IDH1* gene status (mutated vs. wild-type) in 18 histologically proven glioma patients (Pepin et al., 2018). They found an inverse relationship between glioma grade and magnitude |G*|, with higher grade gliomas being softer than low grade tumors. Specifically, magnitude |G*| was lower in grade IV gliomas than grade II tumors but was similar between grade II and grade III gliomas and between grades III and grade IV gliomas. Magnitude |G*| of gliomas was not associated with tumor anatomical location, patient age and tumor volume. With regard to the *IDH1* status, all studied *IDH1* wild-type tumors (n = 12) had lower magnitude |G*| (i.e., were softer) than *IDH1* mutated tumors (n = 6).

3.3. Meningioma

MRE was used in two studies that included only meningioma patients (total of 26 patients) (Hughes et al., 2015; Murphy et al., 2013). A study of 12 patients found that the ratio of $\overline{G'}$ in meningioma relative $\overline{G'}$ in surrounding NAWM correlated positively with the surgeons' qualitative assessment of tumor stiffness as rated on a 5-point scale with possible scores ranging from 1 (soft; 100% removable with suction) to 5 (hard; uniformly hard, requiring ultrasonic aspiration) (Murphy et al., 2013). MRE results showed stronger correlation with surgical assessment of meningioma stiffness when compared with T1w and T2w imaging characteristics.

Hughes and colleagues studied the association of $\overline{G'}$ with intraoperatively evaluated meningioma consistency evaluated according to surgeon impression and durometry findings that were obtained on each surgical specimen taken from different regions of tumor and averaged (Hughes et al., 2015). They found significant and positive correlation between meningioma $\overline{G'}$ with surgeons' impression of tumor stiffness (score range from 1 [removed mostly with suction] to 5 [required scissors or cautery]) and durometer measurements. Furthermore, MRE had high sensitivity, specificity and PPV values for meningioma heterogeneity/homogeneity and hardness that were based on retrospective review of surgical notes.

3.4. Pituitary adenoma

Clinical applications of MRE for estimation of pituitary adenoma stiffness was specifically addressed in one small study of 10 patients with pituitary macroadenomas (Hughes et al., 2016). The authors correlated MRE findings ($\overline{G'}$) with experienced pituitary surgeon's impression of adenoma stiffness (blinded to MRE results) that was classified as either soft (primarily removed with suction), intermediate (parts easily removed with suction but other portions requiring mechanical techniques) or hard (requiring sharp dissection). They found that mean tumor shear stiffness $\overline{G'}$ was significantly lower in soft

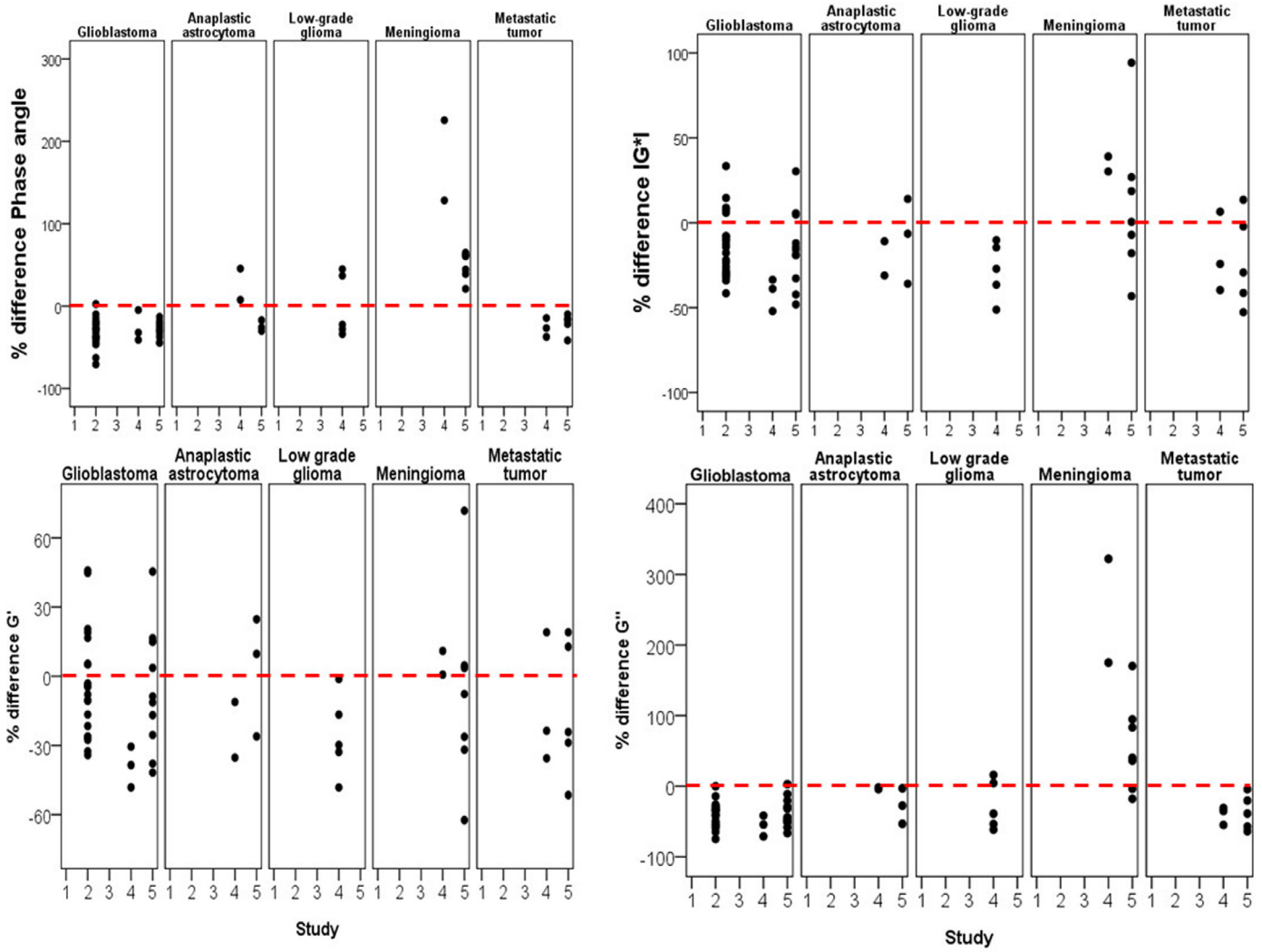

Fig. 4. Percent differences of tumor shear modulus parameters with that of NAWM where the percentage difference is calculated for each individual subject thereby using the subject as its own internal control.

pituitary adenomas when compared to intermediate pituitary adenomas. There were no hard tumors in the series. In 11 pituitary adenoma patients, Sakai and colleagues (Sakai et al., 2016) explored the association of MRE findings with intraoperative tumor consistency as rated on a scale from 1 to 5, with higher scores indicating stiffer tumors. Their data also suggested a tendency for greater shear stiffness $\overline{G'}$ values in patients with firm adenomas (median value of 1.6 kPa) when compared to soft adenomas (median value of 1.1 kPa).

3.5. Pooled Data analysis

Shear stiffness *G'* was available from five studies with a total of 107 brain tumors (Hughes et al., 2016; Reiss-Zimmermann et al., 2015; Sakai et al., 2016; Simon et al., 2013; Streitberger et al., 2014) that included glioblastoma (n = 39), meningioma (n = 22), pituitary adenoma (n = 21), brain metastasis (n = 8), anaplastic astrocytoma (n = 6), vestibular schwannoma (n = 6) and low-grade glioma (n = 5).

Table 2
Tumor to normal appearing white matter percent differences in IG*I, G', G" and Phi across other brain tumor types.

		% difference when compared to NAWM			
Brain tumor diagnosis	N	IG*I	Phase angle	G'	G"
Glioblastoma multiforme	36	−16.52 ± 20.12	−30.53 ± 14.66	−7.28 ± 24.67	−40.51 ± 18.36
Anaplastic astrocytoma	5	−14.06 ± 20.16	−3.99 ± 31.31	−7.62 ± 24.81	−17.90 ± 22.43
Low-grade glioma	5	−34.33 ± 14.10	−0.52 ± 38.15	−25.73 ± 17.71	−26.68 ± 34.88
Meningioma	9	15.68 ± 39.39	78.67 ± 62.45	−4.04 ± 36.74	100.05 ± 107.53
Metastases	8	−21.17 ± 24.35	−23.01 ± 11.39	−14.09 ± 27.23	−38.12 ± 21.06
F-value; *p*-value		4.061; 0.006	25.821; <0.001	0.686; 0.604	18.732; <0.001

Statistically significant differences:.
IG*I: meningioma > glioblastoma (p = =0.06), low grade glioma (p = =0.02) and metastatic tumor (p = =0.02).
Phase angle: Meningioma > glioblastoma, anaplastic astrocytoma, low grade glioma and metastatic tumor (all p-values <0.001).
G": Meningioma > glioblastoma, anaplastic astrocytoma, low grade glioma and metastatic tumor (all p-values <0.001).

Table 3
Overlap coefficients of shear modulus values of glioblastomas, meningiomas, metastatic tumors and normal appearing white matter.

	Glioblastoma	Meningioma	Metastasis
G'			
Meningioma	42.9%	–	–
Metastasis	80.8%	49.4%	–
Normal appearing white matter	74.2%	55.5%	66.4%
IG*I			
Meningioma	42.9%	–	–
Metastasis	82.5%	48.8%	–
Normal appearing white matter	55.4%	85.9%	57.3%
Phase angle			
Meningioma	10.3%	–	–
Metastasis	76.2%	23.2%	–
Normal appearing white matter	46.3%	47.5%	66.7%
G"			
Meningioma	6.3%	–	–
Metastasis	80.9%	15.3%	–
Normal appearing white matter	41.1%	45.2%	54.0%

Three of these studies (n = 63 patients) also reported magnitude |G*| and phase angle φ of NAWM distinct from the brain tumor (Reiss-Zimmermann et al., 2015a; Simon et al., 2013a; Streitberger et al., 2014a).

As demonstrated in **Fig. 3**, there is overlap of the distributions (95% Confidence intervals) of most shear modulus parameters across all histologic tumor types. This is true except when comparing meningiomas and low-grade gliomas with the parameters viscosity G" and phase angle φ. To demonstrate the level of overlap, the overlapping area of normal distributions fit to the data for glioblastomas, meningiomas and metastases as well as for the NAWM data were calculated for each pairing. This overlap probability is reported in **Table 3** and demonstrated substantial overlap between shear modulus values. The lowest overlap coefficients were for φ and G" for meningiomas vs. glioblastomas (10.3% and 6.3%, respectively) and for G" for meningiomas vs. metastases (15.3%).

As discussed earlier, a more robust approach that avoids bias due to different hardware, symmetry assumptions, pulse sequences and reconstruction algorithms, is the comparison of a shear modulus parameter in the tumor to the same parameter in the same subject in NAWM. Note that this approach has also been used by some of the identified studies even when comparing data from a single study where the methodology for all subjects was identical. To this end, we identified data from 63 patients from 3 studies where both brain tumor and NAWM shear modulus parameters were measured. From this data, we calculated ΔG', ΔG", Δ|G*| and $\Delta\varphi$ for different brain tumor diagnoses (**Table 4 and Fig. 4**). ANOVA analyses showed significant differences of mean Δ|G*| (F = 4.061, p = 0.006), mean $\Delta\varphi$ (F = 25.821, $p<0.001$) and mean ΔG" (F = 18.732, $p<0.001$) but not mean ΔG' (F = 0.686, p = 0.6). Post-hoc analyses demonstrates that mean ΔIG*I was greater in meningiomas relative to low grade glioma (p = 0.02) and metastatic tumor (p = 0.02). Mean Δϕ and mean ΔG" were significantly greater in meningioma when compared to glioblastoma, anaplastic astrocytoma, low grade glioma and metastatic tumor (all p-values <0.001). As demonstrated in **Figs. 4 and 5,** meningiomas can be clearly distinguished from gliomas and metastatic brain tumors using $\Delta\varphi$ as all meningiomas having φ greater than NAWM (values above the dashed red line in **Fig. 4**) which was not the case for any other analyzed tumors.

4. Discussion

Interest in MRE for imaging of benign and malignant brain tumors is increasing. Our literature review showed that shear stiffness (G') of meningiomas and pituitary adenomas correlated well with tumor consistency observed intra-operatively. Pooled analyses of reported tumor shear modulus indexes demonstrated significant overlap across different brain tumor diagnoses. However, when analyzing pooled data of tumor to NAWM shear modulus differences obtained from each subject individually, meningiomas had the greatest variability, or range of values, for Δ|G*|, $\Delta\varphi$ and ΔG". In addition, by using $\Delta\varphi$ as a metric, meningiomas as a group could be distinguished from gliomas and metastatic brain tumors as the $\Delta\varphi$ distribution for meningiomas is unipolar positive while for gliomas and metastatic brain tumors it is unipolar negative. Discriminative ability of other shear modulus parameters for different types of brain tumors was limited.

4.1. Surgical considerations

Substantial research efforts were directed towards validating the MRE defined tumor shear stiffness against intraoperatively observed tumor stiffness (Hughes et al., 2016;Murphy et al., 2013; Hughes et al., 2015; Sakai et al., 2016; Xu et al., 2007). In the reviewed studies, intraoperative brain tumor stiffness was graded by the operating neurosurgeons according to personal impression or instruments needed for tumor resection (for example, removable with suction vs. requiring ultrasonic aspiration). Objective intraoperative semi-quantitative estimation of meningioma surgical specimen stiffness using a durometer was performed in one study (Hughes et al., 2015). The reviewed studies indicate that MRE measured shear stiffness G' correlated well with intra-operative stiffness of meningiomas and pituitary adenomas and hence allowed reliable discrimination between stiff and soft meningiomas and pituitary adenomas. Tumor stiffness is among the key characteristics considered for neurosurgical planning, namely selection of surgical approach, resection planning, selection of surgical instruments and anticipation of the intra-operative course (Zada et al., 2013). For example, pituitary adenomas are usually soft tumors that can be totally and safely removed via transsphenoidal surgery. However, in cases of stiff pituitary adenomas, transsphenoidal surgery can be challenging and more extensive surgical approaches, such as craniotomy, should be considered (Zada et al., 2013; 2011). Firm consistency is also among the most important limiting factors of complete resection of intracranial skull base meningiomas (Little et al., 2005; Sekhar et al., 1990). Towards this end, the reviewed studies suggest that MRE can be a valuable tool for discriminating soft vs. firm pituitary adenomas and meningiomas and hence may have value for surgical planning. Larger studies using more objective and reproducible measures of intraoperative tumor should be studied to document validity of MRE for pre-operative prediction of tumor stiffness. The impact of this information for surgical decision making also needs to be addressed in future studies.

Despite substantial research efforts, there are no reliable non-invasive tools for evaluation of brain tumor stiffness preoperatively. Reliable and reproducible quantification of brain tumor stiffness is important for treatment planning, communication across healthcare providers, monitoring changes of tumor stiffness across treatment stages and for consideration of tumor metrics for research studies. Substantial research efforts were directed towards optimizing estimation of brain tumor stiffness using conventional and widely available neuroimaging techniques (MRI and CT). For example, structural T2w and T1w MRI was widely studied for estimating stiffness of meningiomas (Shiroishi et al., 2016; Yao et al., 2018) and pituitary adenomas (Yamamoto et al., 2014; Ma et al., 2016; Romano et al., 2017; Thotakura et al., 2017). A recent review by Shiroishi and colleagues of preoperative imaging studies for prediction of meningioma stiffness concluded that T2w MRI can be a helpful MRI sequence for prediction of meningioma mechanical properties; nevertheless the authors concluded that its reliability warrants further validation (Shiroishi et al., 2016). DTI is another MRI based imaging technique that is promising for evaluation of hardness of meningioma (Romani et al., 2014). Further studies evaluating conventional MRI/CT for evaluation of brain tumor stiffness are warranted.

Table 4
MR elastography studies in animal brain tumor models.

Author, year	Study goal	Model	Major findings
Jamin et al. (2015)	Studied elasticity and viscosity in glioma and metastatic breast cancer models.	Glioma (U-87 MG human glioblastoma cells or RG2 rat glioma cells) and metastatic breast cancer (MDA-MB-231 LM2-4 human triple-negative breast carcinoma cells) female mice models.	All tumors were softer and less viscous than surrounding healthy brain parenchyma. Gliomas derived from U-87 MG were the stiffest and breast cancer metastases (MDA-MB-231 cells) were the softest. Tumor elasticity and viscosity correlated positively with cellular density and microvessel density, but not with extent of collagen deposition nor myelin fiber entrapment.
Schregel et al. (2017)	Explored longitudinal changes of elastic properties in glioblastoma	Glioblastoma stem cell line (G30) established from a patient implanted in five mice. MRE was performed at 2, 3 and 4 weeks post implantation.	Starting from week 2, viscoelastic modulus, shear wave speed and phase angle were significantly lower in tumors when compared with healthy brain tissue. Tumors became softer over time with tumor progression. Tumor heterogeneity increased starting at weeks 3 and 4. Softer tumor regions contained necrosis and patches of viable tumor cells. Dense tumor regions had areas of densely packed tumor cells and blood vessels.
Feng et al. (2016)	Impact of radiotherapy on elasticity of glioblastoma and unaffected brain.	Twelve 7–8 weeks age female Balb/c mice implanted with glioblastoma were randomized to either 20 Gy radiation treatment or no treatment groups.	Shear modulus was lower in tumor relative to mirror brain and decreased over time independently of radiation therapy. Radiation therapy was effective and prolonged mice survival time. Shear modulus of the mirror brain regions remained in treatment group and had increasing trend in not treated animals.

Intra-operative assessment of tumor stiffness is usually a gold standard for estimation of tumor stiffness; however, this type of measurement is invasive, does not allow for pre-surgical planning, and is subjective, therefore at risk for inter-observer variability. Semi-structured neurosurgeon rating scales for quantification of brain tumor stiffness intraoperatively were developed. For example, a five point-intraoperative meningioma consistency grading system was developed by Zada with colleagues aiming to quantify subjective perception of meningioma consistency by evaluating tumor softness/firmness, tumor capsule characteristics and selection of surgical instruments (tumor removal with suction vs. ultrasonic aspiration vs. dissection) needed for tumor debulking (Zada et al., 2013). However, while the scale showed good inter-rated agreement, reliability and clinical utility of this instrument warrants further validation. The association of MRE data with other physical properties of brain tumors that are important for surgical planning and might impact tumor resection strategy and tissue handling characteristics, such as tumor vascularity, rubbery constituency etc., remain to be explored. Also, given relatively small experience but growing interest in MRE for imaging of brain tumor patients, further studies aiming to investigate temporal and inter-institution reliability of MRE are needed before adopting MRE in routine clinical practice.

4.2. Diagnostic considerations

Individual pooled patient level meta-analysis showed that there was substantial overlap of distribution of the reported shear modulus values across different brain tumor diagnoses suggesting that shear modulus indexes have poor discriminative ability across brain tumor diagnoses. However, the ratio of tumor to NAWM shear modulus values seemed to improve discriminative abilities of MRE for meningiomas, suggesting that patient specific rather than absolute shear modulus values should

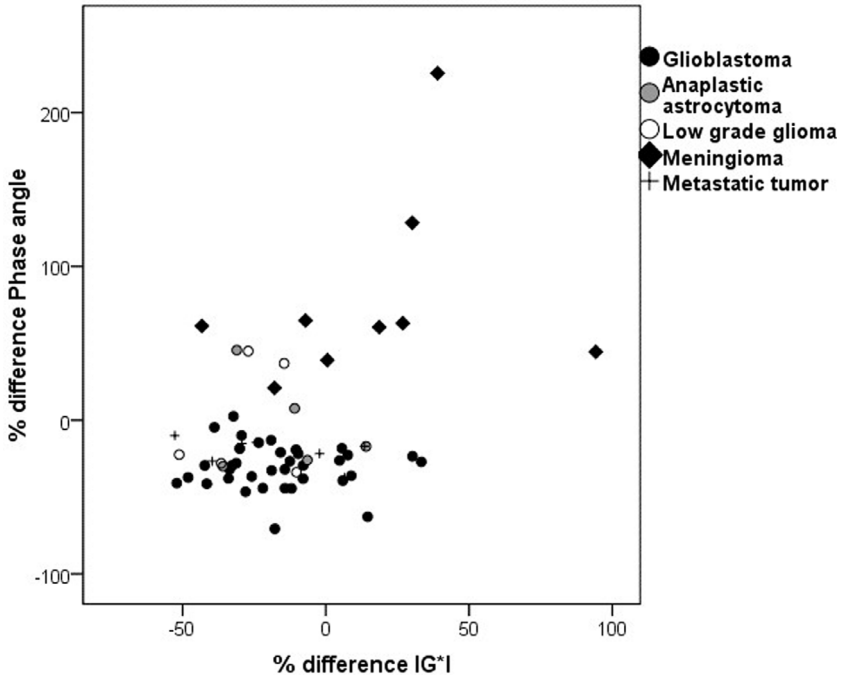

Fig. 5. Scatter plot of tumor to normal appearing white matter percent difference of phase angle and IG*I.

be used. Specifically, meningiomas were stiffer compared to NAWM than gliomas and metastatic tumors and could be distinguished from other brain tumors by $\Delta\phi$ greater than 0. This was not the case for other brain tumor types as there was a substantial overlap of differences of brain tumor to NAWM shear modulus values. Variation of MRE acquisition techniques across studies (i.e. differences in MRI field strength, MRE vibration frequencies, shear modulus reconstruction methods, mechanical coupling devices) can influence the absolute reconstructed shear modulus values between studies. Comparison of tumor to the same patient NAWM shear modulus values allows internal control that removes confounding effect of MRE acquisition techniques for reconstructed shear modulus values. However, pooled data analyses should be also interpreted with caution in the context of small and heterogenous sample sizes across histological diagnoses thus limiting statistical power to detect differences.

A majority of brain tumor types can be reliably distinguished using routine structural MRI modalities based on tumor location, appearance and pattern of contrast enhancement (for example, gliomas vs. meningiomas vs. pituitary adenomas vs. vestibular schwannomas). On the other hand, distinction between brain metastases vs. high-grade gliomas and meningioma vs. vestibular schwannoma can be more challenging in certain clinical scenarios and relying solely on conventional structural MRI sequences. Moreover, sometimes even the differentiation of tumors from inflammatory or demyelinating diseases can be difficult. Biopsy is often required to ultimately establish a diagnosis. Given inconsistency of available evidence, we do not recommend using MRE in the clinical environment for discriminating between different brain tumor entities. Further studies should attempt to investigate additive diagnostic value of MRE in challenging diagnostic scenarios.

Pepin with colleagues found that IDH mutated gliomas were stiffer than IDH wild-type tumors (Pepin et al., 2018), indicating that MRE could potentially hint at one of the molecular signature of gliomas. IDH gene mutation status has a well-defined prognostic significance in gliomas with mutated versions of the gene being associated with a more favorable prognosis relative to the wild-type variant (Yan et al., 2009). These findings remain to be replicated but suggest that MRE measurements could potentially have prognostic significance. Magnetic resonance spectroscopy is another imaging methods that allows not invasive detection 2-hydroxyglurate accumulation that is associated with IDH1 or IDH2 mutation (Choi et al., 2012). It is of interest whether tumor stiffness is associated with other molecular biomarkers of gliomas that have prognostic and therapeutic implications, such as the MGMT gene methylation, mutations in the TERT promoter and codeletion of chromosome arms 1p and 19q (Eckel-Passow et al., 2015; Turkalp et al., 2014). Radiogenomics is a growing field of research that is focused towards identifying noninvasive imaging phenotypes of tumor genetic and molecular characteristics in order to improve diagnostic accuracy and apply personalized treatments (Kickingereder et al., 2016; Smits and van den Bent, 2017). It remains to be seen if integration of MRE imaging data in the radiogenomics models could improve accuracy of imaging signatures of brain tumor molecular/genetic profiles. Also, it will be interesting to see if integration of MRE data in radiomics models could add important prognostic information and improve clinical decision making.

4.3. Shear wave frequency

Shear modulus is expected to increase approximately as the square root of the shear wave frequency (Fabry et al., 2001). While it would be desirable to determine whether or not the data is consistent with the predicted $f^{0.5}$ power law frequency dependence, the frequency dependent factor only amounts to a 6% effect for the two frequencies, 40 and 45 Hz, reported for measurements of G' in glioblastomas and meningiomas. And for pituitary adenomas, where three frequencies were reported, 40, 45 and 60 Hz, the frequency factor between 40 and 60 Hz is 1.22. Both of these factors are well within the range of absolute shifts in G' expected due to other factors such as different groups acquiring their MRE data with different hardware, acquisition protocols, symmetry assumptions, and reconstruction algorithms. This prevents a meaningful comparison of absolute G' values at different frequencies. In addition, for a majority of these studies where multi-frequency behavior is available, control NAWM G' values were not available and hence a comparison of ΔG' between different frequencies, which would potentially eliminate the absolute value biases for different methodologies, was not possible.

4.4. Pre-clinical evidence

Differentiation of glioma progression from radiation necrosis is important to inform clinical decision-making (Nam and de Groot, 2017; Ellingson et al., 2017; Wen et al., 2010) but often remains challenging using conventional imaging techniques (Ellingson et al., 2017; Thust et al., 2018). Longitudinal MRE studies in animal models have provided insights into temporal changes of elastic properties of glioblastoma during disease progression and in response to radiation treatment (**Table 4**) (Feng et al., 2016; Schregel et al., 2017). Schregel and colleagues investigated temporal changes of untreated glioblastoma in an orthotopic mouse model using MRE, and showed that glioblastomas became softer and more heterogenous over time. There was excellent correlation of the MRE-identified softer regions with the tumor necrosis areas (Schregel et al., 2017). Specifically, softer tumor areas contained mostly necrosis with patches of viable tumor cells, while stiffer regions had densely packed tumor cells with blood vessels. Heterogenous elastic properties of glioblastoma were previously described in humans and correspond to commonly observed intraoperative findings of glioblastoma. Another study by Jamin and colleagues in two glioma cell lines (U-87 MG and RG2) and one metastatic breast cancer cells (MDA-MB-231) models in mice also confirmed that MRE findings correlated with tumor cellular and microvascular density, but not with collagen deposition nor myelin fiber entrapment (Jamin et al., 2015). These findings indicate that MRE findings in models of glioblastoma correlate with histological tumor appearance, tumor cell and microvascular density. Studies exploring regional variation of MRE indexes in human patients should be performed. Potentially, MRE could support the evaluation of histological tumor viability and architecture. Furthermore, MRE may have implications for surgical planning to remove a tumor sample with good diagnostic yield. This can be important for deep seated or eloquent brain tumors that are not amenable to extensive surgical resection but are rather deemed only appropriate for a biopsy procedure. MRE may improve the precision spatial location that a biopsy requires.

Temporal and spatial changes of imaging characteristics are important for clinical-decision making and differentiating treatment response, tumor progression and pseudoprogression. We did not find human studies looking into temporal and regional changes of elastic properties of gliomas in response to adjuvant radiotherapy chemotherapy. A study in glioblastoma mice model by Feng and colleagues investigated possible radiation therapy effects (20 Gy) on elastic properties of glioblastoma and healthy brain (Feng et al., 2016). The authors found that shear modulus was lower in brain tumors and that was independent from treatment with radiation therapy that had clear therapeutic benefit. Radiation therapy targeting methods and dosing are different in humans. Therefore, studies in humans looking into possible impact of radiotherapy and chemotherapy on tumor and brain elastic properties will be important to realize clinical impact. Radiation therapy can cause serious toxicity to surrounding brain that ranges from acute encephalopathy to delayed white matter changes, gliosis and vascular lesions (Walker et al., 2014). Chemotherapy induced morphological brain changes include reduced number of glial cells, demyelination, gliosis and leukoencephalopathy (Matsos et al., 2017). We did not find studies exploring the possible impact of chemotherapy on the stiffness of brain tumors and normal appearing white matter;

however, there is evidence to suggest that MRE can be a sensitive method to detect changes in a tissue's mechanical properties in response chemotherapy. For example, a study in a non-Hodgkins lymphoma mouse model documented significant decrease of MRE derived tumor shear stiffness within four days of treatment initiation. This correlated with decreased cellular proliferation, indicating that MRE can be a biomarker of tumor response to chemotherapy (Pepin et al., 2014). MRE can also be an imaging biomarker of response to treatment and treatment—induced necrosis of colon cancer (Jugé et al., 2012; Li et al., 2014). Given documented differences of stiffness in gliomas, gliotic tissue and unaffected brain (Miroshnikova et al., 2016; Moeendarbary et al., 2017) and macroscopic changes of elastic properties of previously irradiated brain areas in glioma patients appreciated intraoperatively, it is possible that therapy-related changes in brain stiffness can be detected with MRE that could be helpful for assessment of response to treatment.

The tumor microenvironment is a pivotal regulator of progression and invasion of gliomas and metastatic brain tumors and is an emerging therapeutic target (Quail and Joyce, 2017). In the brain, the tumor micro-environment is comprised of tumor cells, extracellular matrix (ECM), and non-neoplastic cells, including immune cells and glial cells. Tumor tissue stiffness is an important feature of the tumor microenvironment. ECM pays an important role for invasion and progression of glioma cells (Foty, 2013; Lu et al., 2012; Ulrich et al., 2009). Stiffness of ECM has been shown to affect glioma cell migration and proliferation (Ulrich et al., 2009). Specifically, glioma cells spread more extensively and rapidly on rigid extracellular matrix and glioma cell migration decreased with decreasing rigidity of ECM (Ulrich et al., 2009). Stiffness also can be an important biomarker of glioma growth and response to therapy. It was recently demonstrated that higher stiffness of ECM in gliomas was associated with higher glioma grade and more aggressive behavior (Miroshnikova et al., 2016) indicating that ECM stiffness has prognostic importance. A recent pre—clinical study demonstrated that MRE can be a valuable biomarker of ECM stiffness of brain tumors (Li et al., 2019). Towards this end, further studies should investigate whether glioma stiffness measured with MRE can be used to describe tumor microenvironment and serve as a biomarker of tumor behavior and response to chemotherapy.

5. Conclusions

Potential clinical applications of MRE for imaging of benign and malignant brain tumors are increasingly studied. Several studies have showed that the quantitative shear stiffness (G') of meningiomas and pituitary adenomas as measured with MRE correlate well with the intra-operatively assessed subjective evaluation of tumor consistency of the surgeon indicating that MRE may be a promising technique for surgical planning. On the other hand, discrimination between different tumor types based on the shear modulus value itself is not currently possible because of substantial overlap of the distributions of each of the shear modulus parameters from different tumors as well as NAWM (**Fig. 3**). To remove any bias in the reported values of the shear modulus parameters due the particular type of hardware, reconstruction methodology and SNR, we computed the difference in each shear modulus parameter in the tumor and that of the same individual's contralateral NAWM: ΔG', ΔG", Δ|G*|, and $\Delta\varphi$ (**Fig. 4**). This resulted in some improvement in defining the distribution of values in different tumors. In addition, for a neurosurgeon, it is important to determine prior to surgery the shear modulus value of the tumor compared to that of NAWM in that specific subject. For the pooled meta-analysis performed here, we see that for most brain tumor types the difference ΔG" between the viscosity of the tumor (G") and the viscosity of NAWM in the same patient (i.e. using the patient's NAWM as a control), is either positive or negative, i.e. the distribution of ΔG" values lies either above or below the red-dashed "zero difference" line in **Fig. 4**. Thus, while there still remains considerable heterogeneity of the ΔG" values from different individuals having the same type of tumor, there is now a predominant sign (either positive or negative) for ΔG". Furthermore, the distribution of ΔG" values in meningiomas is unique in that it is the only distribution with a predominantly unipolar positive distribution. If, after more extensive data becomes available, a further pooled analysis shows that the distribution of ΔG" values in meningiomas is indeed uniquely unipolar positive, one could then predict with confidence whether or not the tumor type is a meningioma based on an MRE exam.

Nevertheless, even after normalizing the tumor data with respect to the individual's own contralateral NAWM, **Fig. 4** still shows a wide range of values for essentially all tumors and all parameters. Before the adoption of MRE into routine clinical practice, it is important to establish its reproducibility as an imaging biomarker of cancer (O'Connor et al., 2017; Sullivan et al., 2015). Certainly, more data of tumor and contralateral NAWM shear modulus values need to be acquired and accumulated in the literature so that one can be more confident of the distribution of the shear modulus values. In addition, it seems it may be wise to consider recording additional subject data that may influence tumor stiffness and viscosity in order to eventually be able narrow these distributions. For example, it is well known that tumors (i) increase their size over time, (ii) are typically spatially inhomogeneous, and (iii) that the spatial pattern of inhomogeneity can change over time. Perhaps a measure of tumor size/age and heterogeneity may be useful in this regard to eventually make these measurements useful for diagnostic and therapeutic follow up purposes. Finally, further technological improvements with the goal of unification of MRE techniques and protocols is encouraged as well as studies evaluating accuracy, clinical applicability, correlation with treatment-related changes and biological correlates of MRE.

Declaration of Competing Interest

None.

Acknowledgement

We gratefully acknowledge support from NIH R21 EB030757, NIH P411EB015898 and NCIGT The National Center for Image Guided Therapy P41EB015898, the European Union's Horizon 2020 Research and Innovation program under grant agreement No 668039, Brigham and Women's Hospital Department of Radiology.

References

Almenawer, S.A., Badhiwala, J.H., Alhazzani, W., Greenspoon, J., Farrokhyar, F., Yarascavitch, B., Algird, A., Kachur, E., Cenic, A., Sharieff, W., Klurfan, P., Gunnarsson, T., Ajani, O., Reddy, K., Singh, S.K., Murty, N.K., 2015. Biopsy versus partial versus gross total resection in older patients with high-grade glioma: a systematic review and meta-analysis. Neuro-Oncol. 17, 868–881. https://doi.org/10.1093/neuonc/nou349.

Chauvet, D., Imbault, M., Capelle, L., Demene, C., Mossad, M., Karachi, C., Boch, A.-L., Gennisson, J.-L., Tanter, M., 2016. In vivo measurement of brain tumor elasticity using intraoperative shear wave elastography. Ultraschall Med. Stuttg. Ger. 1980 37, 584–590. https://doi.org/10.1055/s-0034-1399152.

Choi, C., Ganji, S.K., DeBerardinis, R.J., Hatanpaa, K.J., Rakheja, D., Kovacs, Z., Yang, X.-L., Mashimo, T., Raisanen, J.M., Marin-Valencia, I., Pascual, J.M., Madden, C.J., Mickey, B.E., Malloy, C.M., Bachoo, R., Maher, E.A., 2012. 2-hydroxyglutarate detection by magnetic resonance spectroscopy in IDH-mutated glioma patients. Nat. Med. 18, 624–629. https://doi.org/10.1038/nm.2682.

Eckel-Passow, J.E., Lachance, D.H., Molinaro, A.M., Walsh, K.M., Decker, P.A., Sicotte, H., Pekmezci, M., Rice, T., Kosel, M.L., Smirnov, I.V., Sarkar, G., Caron, A.A., Kollmeyer, T.M., Praska, C.E., Chada, A.R., Halder, C., Hansen, H.M., McCoy, L.S., Bracci, P.M., Marshall, R., Zheng, S., Reis, G.F., Pico, A.R., O'Neill, B.P., Buckner, J.C., Giannini, C., Huse, J.T., Perry, A., Tihan, T., Berger, M.S., Chang, S.M., Prados, M.D., Wiemels, J., Wiencke, J.K., Wrensch, M.R., Jenkins, R.B., 2015. Glioma groups based on 1p/19q, *IDH*, and *tert* promoter mutations in tumors. N. Engl. J. Med. 372, 2499–2508. https://doi.org/10.1056/NEJMoa1407279.

Ellingson, B.M., Chung, C., Pope, W.B., Boxerman, J.L., Kaufmann, T.J., 2017. Pseudoprogression, radionecrosis, inflammation or true tumor progression? challenges associated with glioblastoma response assessment in an evolving therapeutic landscape. J. Neurooncol 134, 495–504. https://doi.org/10.1007/s11060-017-2375-2.

Expert Panel on Gastrointestinal Imaging:, J.M.,Horowitz, J.M., Kamel, I.R., Arif-Tiwari, H., Asrani, S.K., Hindman, N.M., Kaur, H., McNamara, M.M., Noto, R.B., Qayyum, A., Lalani, T., 2017. ACR appropriateness criteria® chronic liver disease. J. am. coll. radiol. JACR 14, S103–S117. https://doi.org/10.1016/j.jacr.2017.02.011.

Fabry, B., Maksym, G.N., Butler, J.P., Glogauer, M., Navajas, D., Fredberg, J.J., 2001. Scaling the microrheology of living cells. Phys. Rev. Lett. 87, 148102.

Feng, Y., Clayton, E.H., Okamoto, R.J., Engelbach, J., Bayly, P.V., Garbow, J.R., 2016. A longitudinal magnetic resonance elastography study of murine brain tumors following radiation therapy. Phys. Med. Biol. 61, 6121–6131. https://doi.org/10.1088/0031-9155/61/16/6121.

Foty, R.A., 2013. Tumor cohesion and glioblastoma cell dispersal. Future Oncol. Lond. Engl. 9, 1121–1132. https://doi.org/10.2217/fon.13.66.

Hiscox, L.V., Johnson, C.L., Barnhill, E., McGarry, M.D.J., Huston, J., van Beek, E.J.R., Starr, J.M., Roberts, N., 2016. Magnetic resonance elastography (MRE) of the human brain: technique, findings and clinical applications. Phys. Med. Biol. 61, R401–R437. https://doi.org/10.1088/0031-9155/61/24/R401.

Hughes, J.D., Fattahi, N., Van Gompel, J., Arani, A., Ehman, R., Huston, J., 2016. Magnetic resonance elastography detects tumoral consistency in pituitary macroadenomas. Pituitary 19, 286–292. https://doi.org/10.1007/s11102-016-0706-5.

Hughes, J.D., Fattahi, N., Van Gompel, J., Arani, A., Meyer, F., Lanzino, G., Link, M.J., Ehman, R., Huston, J., 2015. Higher-Resolution Magnetic Resonance Elastography in Meningiomas to Determine Intratumoral Consistency. Neurosurgery 77, 653–658. https://doi.org/10.1227/NEU.0000000000000892.

Itamura, K., Chang, K.-.E., Lucas, J., Donoho, D.A., Giannotta, S., Zada, G., 2018. Prospective clinical validation of a meningioma consistency grading scheme: association with surgical outcomes and extent of tumor resection. J. Neurosurg 1–5. https://doi.org/10.3171/2018.7.JNS1838.

Jamin, Y., Boult, J.K.R., Li, J., Popov, S., Garteiser, P., Ulloa, J.L., Cummings, C., Box, G., Eccles, S.A., Jones, C., Waterton, J.C., Bamber, J.C., Sinkus, R., Robinson, S.P., 2015. Exploring the biomechanical properties of brain malignancies and their pathologic determinants in vivo with magnetic resonance elastography. Cancer Res. 75, 1216–1224. https://doi.org/10.1158/0008-5472.CAN-14-1997.

Jugé, L., Doan, B.-T., Seguin, J., Albuquerque, M., Larrat, B., Mignet, N., Chabot, G.G., Scherman, D., Paradis, V., Vilgrain, V., Van Beers, B.E., Sinkus, R., 2012. Colon tumor growth and antivascular treatment in mice: complementary assessment with mr elastography and diffusion-weighted MR imaging. Radiology 264, 436–444. https://doi.org/10.1148/radiol.12111548.

Kickingereder, P., Bonekamp, D., Nowosielski, M., Kratz, A., Sill, M., Burth, S., Wick, A., Eidel, O., Schlemmer, H.-P., Radbruch, A., Debus, J., Herold-Mende, C., Unterberg, A., Jones, D., Pfister, S., Wick, W., von Deimling, A., Bendszus, M., Capper, D., 2016. Radiogenomics of glioblastoma: machine learning–based classification of molecular characteristics by using multiparametric and multiregional mr imaging features. Radiology 281, 907–918. https://doi.org/10.1148/radiol.2016161382.

Kim, Y.S., Jang, Y.N., Song, J.S., 2018. Comparison of gradient-recalled echo and spin-echo echo-planar imaging MR elastography in staging liver fibrosis: a meta-analysis. Eur. Radiol. 28, 1709–1718. https://doi.org/10.1007/s00330-017-5149-5.

Li, J., Jamin, Y., Boult, J.K.R., Cummings, C., Waterton, J.C., Ulloa, J., Sinkus, R., Bamber, J.C., Robinson, S.P., 2014. Tumour biomechanical response to the vascular disrupting agent ZD6126 in vivo assessed by magnetic resonance elastography. Br. J. Cancer 110, 1727–1732. https://doi.org/10.1038/bjc.2014.76.

Li, J., Zormpas-Petridis, K., Boult, J.K.R., Reeves, E.L., Heindl, A., Vinci, M., Lopes, F., Cummings, C., Springer, C.J., Chesler, L., Jones, C., Bamber, J.C., Yuan, Y., Sinkus, R., Jamin, Y., Robinson, S.P., 2019. Investigating the contribution of collagen to the tumor biomechanical phenotype with noninvasive magnetic resonance elastography. Cancer Res. https://doi.org/10.1158/0008-5472.CAN-19-1595.

Li, S., Chen, M., Wang, W., Zhao, W., Wang, J., Zhao, X., Zhou, C., 2011. A feasibility study of MR elastography in the diagnosis of prostate cancer at 3.0T. Acta Radiol. 52, 354–358. https://doi.org/10.1258/ar.2010.100276.

Little, K.M., Friedman, A.H., Sampson, J.H., Wanibuchi, M., Fukushima, T., 2005. Surgical management of petroclival meningiomas: defining resection goals based on risk of neurological morbidity and tumor recurrence rates in 137 patients. Neurosurgery 56, 546–559 discussion 546-59.

Lu, P., Weaver, V.M., Werb, Z., 2012. The extracellular matrix: a dynamic niche in cancer progression. J. Cell Biol. 196, 395–406. https://doi.org/10.1083/jcb.201102147.

Lu, V.M., Jue, T.R., McDonald, K.L., Rovin, R.A., 2018. The survival effect of repeat surgery at glioblastoma recurrence and its trend: a systematic review and meta-analysis. World Neurosurg. 115, 453–459. https://doi.org/10.1016/j.wneu.2018.04.016.

Ma, Z., He, W., Zhao, Y., Yuan, J., Zhang, Q., Wu, Y., Chen, H., Yao, Z., Li, S., Wang, Y., 2016. Predictive value of pwi for blood supply and T1-spin echo mri for consistency of pituitary adenoma. Neuroradiology 58, 51–57. https://doi.org/10.1007/s00234-015-1591-8.

Matsos, A., Loomes, M., Zhou, I., Macmillan, E., Sabel, I., Rotziokos, E., Beckwith, W., Johnston, I.N., 2017. Chemotherapy-induced cognitive impairments: white matter pathologies. Cancer Treat. Rev 61, 6–14. https://doi.org/10.1016/j.ctrv.2017.09.010.

Miroshnikova, Y.A., Mouw, J.K., Barnes, J.M., Pickup, M.W., Lakins, J.N., Kim, Y., Lobo, K., Persson, A.I., Reis, G.F., McKnight, T.R., Holland, E.C., Phillips, J.J., Weaver, V.M., 2016. Tissue mechanics promote IDH1-dependent HIF1α–tenascin c feedback to regulate glioblastoma aggression. Nat. Cell Biol. 18, 1336–1345. https://doi.org/10.1038/ncb3429.

Moeendarbary, E., Weber, I.P., Sheridan, G.K., Koser, D.E., Soleman, S., Haenzi, B., Bradbury, E.J., Fawcett, J., Franze, K., 2017. The soft mechanical signature of glial scars in the central nervous system. Nat. Commun. 8, 14787. https://doi.org/10.1038/ncomms14787.

Murphy, M.C., Huston, J., Ehman, R.L., 2017. MR elastography of the brain and its application in neurological diseases. NeuroImage. https://doi.org/10.1016/j.neuroimage.2017.10.008.

Murphy, M.C., Huston, J., Glaser, K.J., Manduca, A., Meyer, F.B., Lanzino, G., Morris, J.M., Felmlee, J.P., Ehman, R.L., 2013. Preoperative assessment of meningioma stiffness using magnetic resonance elastography. J. Neurosurg. 118, 643–648. https://doi.org/10.3171/2012.9.JNS12519.

Muthupillai, R., Lomas, D.J., Rossman, P.J., Greenleaf, J.F., Manduca, A., Ehman, R.L., 1995. Magnetic resonance elastography by direct visualization of propagating acoustic strain waves. Science 269, 1854–1857.

Nam, J.Y., de Groot, J.F., 2017. Treatment of glioblastoma. J. Oncol. Pract. 13, 629–638. https://doi.org/10.1200/JOP.2017.025536.

O'Connor, J.P.B., Aboagye, E.O., Adams, J.E., Aerts, H.J.W.L., Barrington, S.F., Beer, A.J., Boellaard, R., Bohndiek, S.E., Brady, M., Brown, G., Buckley, D.L., Chenevert, T.L., Clarke, L.P., Collette, S., Cook, G.J., deSouza, N.M., Dickson, J.C., Dive, C., Evelhoch, J.L., Faivre-Finn, C., Gallagher, F.A., Gilbert, F.J., Gillies, R.J., Goh, V., Griffiths, J.R., Groves, A.M., Halligan, S., Harris, A.L., Hawkes, D.J., Hoekstra, O.S., Huang, E.P., Hutton, B.F., Jackson, E.F., Jayson, G.C., Jones, A., Koh, D.-.M., Lacombe, D., Lambin, P., Lassau, N., Leach, M.O., Lee, T.-.Y., Leen, E.L., Lewis, J.S., Liu, Y., Lythgoe, M.F., Manoharan, P., Maxwell, R.J., Miles, K.A., Morgan, B., Morris, S., Ng, T., Padhani, A.R., Parker, G.J.M., Partridge, M., Pathak, A.P., Peet, A.C., Punwani, S., Reynolds, A.R., Robinson, S.P., Shankar, L.K., Sharma, R.A., Soloviev, D., Stroobants, S., Sullivan, D.C., Taylor, S.A., Tofts, P.S., Tozer, G.M., van Herk, M., Walker-Samuel, S., Wason, J., Williams, K.J., Workman, P., Yankeelov, T.E., Brindle, K.M., McShane, L.M., Jackson, A., Waterton, J.C., 2017. Imaging biomarker roadmap for cancer studies. Nat. Rev. Clin. Oncol. 14, 169–186. https://doi.org/10.1038/nrclinonc.2016.162.

Pepin, K.M., Chen, J., Glaser, K.J., Mariappan, Y.K., Reuland, B., Ziesmer, S., Carter, R., Ansell, S.M., Ehman, R.L., McGee, K.P., 2014. MR elastography derived shear stiffness-a new imaging biomarker for the assessment of early tumor response to chemotherapy. Magn. Reson. Med. 71, 1834–1840. https://doi.org/10.1002/mrm.24825.

Pepin, K.M., McGee, K.P., Arani, A., Lake, D.S., Glaser, K.J., Manduca, A., Parney, I.F., Ehman, R.L., Huston, J., 2018. MR elastography analysis of glioma stiffness and IDH1-mutation status. AJNR Am. J. Neuroradiol. 39, 31–36. https://doi.org/10.3174/ajnr.A5415.

Quail, D.F., Joyce, J.A., 2017. The microenvironmental landscape of brain tumors. Cancer Cell 31, 326–341. https://doi.org/10.1016/j.ccell.2017.02.009.

Reiss-Zimmermann, M., Streitberger, K.-.J., Sack, I., Braun, J., Arlt, F., Fritzsch, D., Hoffmann, K.-.T., 2015. High resolution imaging of viscoelastic properties of intracranial tumours by multi-frequency magnetic resonance elastography. Clin. Neuroradiol. 25, 371–378. https://doi.org/10.1007/s00062-014-0311-9.

Rizk, A.R., Adam, A., Gugel, I., Schittenhelm, J., Tatagiba, M., Ebner, F.H., 2017. Implications of vestibular schwannoma consistency: analysis of 140 cases regarding radiologic and clinical features. World Neurosurg 99, 159–163. https://doi.org/10.1016/j.wneu.2016.11.082.

Romani, R., Tang, W.-.J., Mao, Y., Wang, D.-.J., Tang, H.-.L., Zhu, F.-.P., Che, X.-.M., Gong, Y., Zheng, K., Zhong, P., Li, S.-.Q., Bao, W.-.M., Benner, C., Wu, J.-.S., Zhou, L.-.F., 2014. Diffusion tensor magnetic resonance imaging for predicting the consistency of intracranial meningiomas. Acta Neurochir. (Wien) 156, 1837–1845. https://doi.org/10.1007/s00701-014-2149-y.

Romano, A., Coppola, V., Lombardi, M., Lavorato, L., Di Stefano, D., Caroli, E., Rossi Espagnet, M.C., Tavanti, F., Minniti, G., Trillò, G., Bozzao, A., 2017. Predictive role of dynamic contrast enhanced T1-weighted mr sequences in pre-surgical evaluation of macroadenomas consistency. Pituitary 20, 201–209. https://doi.org/10.1007/s11102-016-0760-z.

Sakai, N., Takehara, Y., Yamashita, S., Ohishi, N., Kawaji, H., Sameshima, T., Baba, S., Sakahara, H., Namba, H., 2016. Shear stiffness of 4 common intracranial tumors measured using mr elastography: comparison with intraoperative consistency grading. AJNR Am. J. Neuroradiol. 37, 1851–1859. https://doi.org/10.3174/ajnr.A4832.

Schregel, K., Nazari, N., Nowicki, M.O., Palotai, M., Lawler, S.E., Sinkus, R., Barbone, P.E., Patz, S., 2017. Characterization of glioblastoma in an orthotopic mouse model with magnetic resonance elastography. NMR Biomed. https://doi.org/10.1002/nbm.3840.

Sekhar, L.N., Jannetta, P.J., Burkhart, L.E., Janosky, J.E., 1990. Meningiomas involving the clivus: a six-year experience with 41 patients. Neurosurgery 27, 764–781 discussion 781.

Shiroishi, M.S., Cen, S.Y., Tamrazi, B., D'Amore, F., Lerner, A., King, K.S., Kim, P.E., Law, M., Hwang, D.H., Boyko, O.B., Liu, C.-S.J., 2016. Predicting meningioma consistency on preoperative neuroimaging studies. Neurosurg. Clin. N. Am. 27, 145–154. https://doi.org/10.1016/j.nec.2015.11.007.

Siegmann, K.C., Xydeas, T., Sinkus, R., Kraemer, B., Vogel, U., Claussen, C.D., 2010. Diagnostic value of MR elastography in addition to contrast-enhanced MR imaging of the breast—initial clinical results. Eur. Radiol. 20, 318–325. https://doi.org/10.1007/s00330-009-1566-4.

Simon, M., Guo, J., Papazoglou, S., Scholand-Engler, H., Erdmann, C., Melchert, U., Bonsanto, M., Braun, J., Petersen, D., Sack, I., Wuerfel, J., 2013. Non-invasive characterization of intracranial tumors by magnetic resonance elastography. New J. Phys. 15, 085024. https://doi.org/10.1088/1367-2630/15/8/085024.

Smits, M., van den Bent, M.J., 2017. Imaging correlates of adult glioma genotypes. Radiology 284, 316–331. https://doi.org/10.1148/radiol.2017151930.

Streitberger, K.-J., Reiss-Zimmermann, M., Freimann, F.B., Bayerl, S., Guo, J., Arlt, F., Wuerfel, J., Braun, J., Hoffmann, K.-T., Sack, I., 2014. High-resolution mechanical imaging of glioblastoma by multifrequency magnetic resonance elastography. PLoS ONE 9, e110588. https://doi.org/10.1371/journal.pone.0110588.

Sullivan, D.C., Obuchowski, N.A., Kessler, L.G., Raunig, D.L., Gatsonis, C., Huang, E.P.,

Kondratovich, M., McShane, L.M., Reeves, A.P., Barboriak, D.P., Guimaraes, A.R., Wahl, R.L., Metrology Working Group, R.S.N.A.-Q.I.B.A., 2015. Metrology standards for quantitative imaging biomarkers. Radiology 277, 813–825. https://doi.org/10.1148/radiol.2015142202.

Thompson, S.M., Wang, J., Chandan, V.S., Glaser, K.J., Roberts, L.R., Ehman, R.L., Venkatesh, S.K., 2017. MR elastography of hepatocellular carcinoma: correlation of tumor stiffness with histopathology features—Preliminary findings. Magn. Reson. Imaging 37, 41–45. https://doi.org/10.1016/j.mri.2016.11.005.

Thotakura, A.K., Patibandla, M.R., Panigrahi, M.K., Mahadevan, A., 2017. Is it really possible to predict the consistency of a pituitary adenoma preoperatively? Neurochirurgie 63, 453–457. https://doi.org/10.1016/j.neuchi.2017.06.003.

Thust, S.C., van den Bent, M.J., Smits, M., 2018. Pseudoprogression of brain tumors. J. Magn. Reson. Imaging. https://doi.org/10.1002/jmri.26171.

Turkalp, Z., Karamchandani, J., Das, S., 2014. *IDH* mutation in glioma. JAMA Neurol 71, 1319. https://doi.org/10.1001/jamaneurol.2014.1205.

Ulrich, T.A., de Juan Pardo, E.M., Kumar, S., 2009. The mechanical rigidity of the extracellular matrix regulates the structure, motility, and proliferation of glioma cells. Cancer Res 69, 4167–4174. https://doi.org/10.1158/0008-5472.CAN-08-4859.

Walker, A.J., Ruzevick, J., Malayeri, A.A., Rigamonti, D., Lim, M., Redmond, K.J., Kleinberg, L., 2014. Postradiation imaging changes in the CNS: how can we differentiate between treatment effect and disease progression? Future Oncol. Lond. Engl 10, 1277–1297. https://doi.org/10.2217/fon.13.271.

Wen, P.Y., Macdonald, D.R., Reardon, D.A., Cloughesy, T.F., Sorensen, A.G., Galanis, E., Degroot, J., Wick, W., Gilbert, M.R., Lassman, A.B., Tsien, C., Mikkelsen, T., Wong, E.T., Chamberlain, M.C., Stupp, R., Lamborn, K.R., Vogelbaum, M.A., van den Bent, M.J., Chang, S.M., 2010. Updated response assessment criteria for high-grade gliomas: response assessment in neuro-oncology working group. J. Clin. Oncol. Off. J. Am. Soc. Clin. Oncol. 28, 1963–1972. https://doi.org/10.1200/JCO.2009.26.3541.

Xia, L., Fang, C., Chen, G., Sun, C., 2018. Relationship between the extent of resection and the survival of patients with low-grade gliomas: a systematic review and meta-analysis. BMC Cancer 18, 48. https://doi.org/10.1186/s12885-017-3909-x.

Xu, L., Lin, Y., Han, J.C., Xi, Z.N., Shen, H., Gao, P.Y., 2007. Magnetic resonance elastography of brain tumors: preliminary results. Acta Radiol. Stockh. Swed. 1987 48, 327–330. https://doi.org/10.1080/02841850701199967.

Yamamoto, J., Kakeda, S., Shimajiri, S., Takahashi, M., Watanabe, K., Kai, Y., Moriya, J., Korogi, Y., Nishizawa, S., 2014. Tumor consistency of pituitary macroadenomas: predictive analysis on the basis of imaging features with contrast-enhanced 3D fiesta at 3T. Am. J. Neuroradiol. 35, 297–303. https://doi.org/10.3174/ajnr.A3667.

Yan, H., Parsons, D.W., Jin, G., McLendon, R., Rasheed, B.A., Yuan, W., Kos, I., Batinic-Haberle, I., Jones, S., Riggins, G.J., Friedman, H., Friedman, A., Reardon, D., Herndon, J., Kinzler, K.W., Velculescu, V.E., Vogelstein, B., Bigner, D.D., 2009. *IDH1* and *IDH2* mutations in gliomas. N. Engl. J. Med 360, 765–773. https://doi.org/10.1056/NEJMoa0808710.

Yao, A., Pain, M., Balchandani, P., Shrivastava, R.K., 2018. Can mri predict meningioma consistency?: a correlation with tumor pathology and systematic review. Neurosurg. Rev. 41, 745–753. https://doi.org/10.1007/s10143-016-0801-0.

Yiping, L., Ji, X., Daoying, G., Bo, Y., 2016. Prediction of the consistency of pituitary adenoma: a comparative study on diffusion-weighted imaging and pathological results. J. Neuroradiol. 43, 186–194. https://doi.org/10.1016/j.neurad.2015.09.003.

Zada, G., Du, R., Laws, E.R., 2011. Defining the “edge of the envelope”: patient selection in treating complex sellar-based neoplasms via transsphenoidal versus open craniotomy. J. Neurosurg. 114, 286–300. https://doi.org/10.3171/2010.8.JNS10520.

Zada, G., Yashar, P., Robison, A., Winer, J., Khalessi, A., Mack, W.J., Giannotta, S.L., 2013. A proposed grading system for standardizing tumor consistency of intracranial meningiomas. Neurosurg. Focus 35, E1. https://doi.org/10.3171/2013.8.FOCUS13274.